

Phonons and spin waves in the magnetic semiconductor chalcopyrite CuFeS_2

M. J. Harris

ISIS Facility, Rutherford Appleton Laboratory, Chilton, Didcot, Oxon, OX11 0QX, United Kingdom

M. P. Zinkin

Oxford Physics, Clarendon Laboratory, Parks Road, Oxford, OX1 3PU, United Kingdom

I. P. Swainson

Neutron and Condensed Matter Science Branch, AECL Research, Chalk River Laboratories, Chalk River, Ontario, K0J 1J0, Canada

(Received 14 August 1996)

We present the results of inelastic neutron-scattering measurements of the spin wave and phonon dispersion in the antiferromagnetic semiconductor chalcopyrite CuFeS_2 . The spin waves are steeply dispersive, and are described well by a simple local-moment model that considers only nearest-neighbor interactions. The nearest-neighbor exchange energy is determined as 2.27(2) THz, and there is an anisotropy gap of 1.28(1) THz. [S0163-1829(97)03911-8]

Chalcopyrite (CuFeS_2) is a semiconducting material with unusual properties, especially compared with related semiconductors with the chalcopyrite structure, such as CuGaSe_2 and AgInS_2 . The optical absorption edge is only at about 0.5 eV (Ref. 1) and the electrical conductivity is anomalously low, even though the carrier concentration is high.² It is thought that the explanation lies in the fact that chalcopyrite is magnetically ordered. Chalcopyrite displays magnetic properties that are reminiscent of a metal: it orders antiferromagnetically with the very high Néel temperature of 823 K, and the magnetic susceptibility is relatively temperature independent.² The magnetic structure of chalcopyrite was among the earliest to be determined using neutron diffraction,³ and it was found to be a simple antiferromagnet, with every Fe atom tetrahedrally coordinated to four others through bonds to S atoms, and the moments ordered antiparallel along the c axis. The effective magnetic moment of the Fe atom was determined from the neutron diffraction data to be $3.85\mu_B$. This value corresponds to neither that for Fe^{2+} nor that for Fe^{3+} , while the magnetic moment of the Cu atom is zero, or $0.2\mu_B$ at the most.³ These properties presumably arise from delocalization of the $3d$ electrons, which form the main part of the upper valence band.⁴

Mikhailovskii *et al.*⁵ have suggested that the reason for the unusually low electrical conductivity is that strong coupling occurs between the charge carriers and the magnetic moments. The idea is that a carrier orients the surrounding magnetic moments parallel to its own spin to give rise to a mobile ferromagnetic domain consisting of perhaps 15 to 20 spins at room temperature; this is commonly known as a spin polaron. This concept is given credence by the fact that the conductivity rises dramatically upon heating above the Néel temperature,² as would be expected from the decrease in effective mass of the charge carriers as they become decoupled from the relatively rigid antiferromagnetic structure.

In this paper, we present an inelastic neutron-scattering study of the phonon and spin dynamics of chalcopyrite under ambient conditions, with the aim of determining the nature of the structural and magnetic interactions. The phonon mea-

surements were only partially successful, and are presented here for completeness, but with the spin-wave measurements we were able to analyze our data with a local-moment model and to extract the magnitude of the exchange interaction.

Since high-purity synthetic crystals of chalcopyrite are not available, we used a natural single crystal from the Wheal Unity Mine in Cornwall that was supplied by the Natural History Museum (London), with the registered number BM41087. This crystal has a volume of approximately 2 cm^3 , and a mosaic spread of approximately 1.7° .

Inelastic neutron-scattering measurements were performed on the E3 triple-axis spectrometer at the NRU reactor at Chalk River Laboratories. Two spectrometer configurations were used: for energy transfers below 4 THz, the monochromator and analyzer were both pyrolytic graphite (002) planes and the analyzing energy was fixed at 3.11 THz; for energy transfers above 4 THz, the monochromator was changed to beryllium—with the (002) planes—and the analyzing energy was fixed at 8.23 THz. These two analyzing energies were carefully chosen to optimize the instrumental resolution and range of accessible energy transfers within the particular kinematic constraints of the spectrometer (which has a restricted range of monochromator take-off angles). At the same time, these two analyzing energies allowed for the use of a pyrolytic graphite filter in the scattered beam to remove spurious higher-order scattering. In both cases, the in-plane collimation was $60'-24'-33'-150'$. The crystal was held in the beam with an aluminum peg, shielded with cadmium, and all measurements were performed with the sample at room temperature.

The crystal was aligned so that the scattering plane contained $(h\ h\ l)$ wave vectors. The space group of chalcopyrite is $I42d$, which means that the systematic absences for nuclear reflections in this scattering plane are $2h+l=4n$. Measurements of the spin waves were performed at the (002), (110), (114), and (006) reciprocal lattice positions, which are positions of zero nuclear Bragg scattering, but are magnetic zone centers. We found that the spin waves are very steeply dispersive, so we characterized them mostly

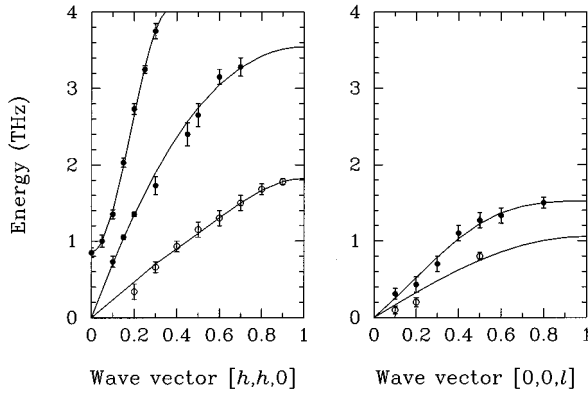


FIG. 1. Measured phonon dispersion in chalcopyrite for $[\xi \xi 0]$ and $[0 0 \xi]$ wave vectors. Open circles denote observed phonon peaks with transverse polarization, full circles denote longitudinal polarization. The curves are guides to the eye.

with constant-energy scans at a number of energies up to 17 THz. However, because of the combined effects of the low incident neutron flux at these relatively high energies, and a high background due to the low scattering angles required, we found that the maximum energy transfer at which reliable data were obtained was 12 THz.

In addition to the spin-wave measurements, we also performed constant- Q scans around the $(2 2 0)$, $(0 0 4)$, and $(0 0 8)$ nuclear Bragg peaks, in order to investigate the phonon dispersion of chalcopyrite. We observed a number of dispersive excitations that we interpret as phonons, since they emanate from nuclear zone centers and appear roughly to strengthen in zones going further out in reciprocal space. As stated above, these measurements were only partially successful due to poor phonon intensities, particularly for scans around the $(0 0 4)$ peak, which were used to determine the phonons for $[0 0 l]$ wave vectors. We present all of the measured phonon dispersion curves in Fig. 1. For both directions we observed a transverse acoustic branch and a longitudinal acoustic branch, while for $[h h 0]$ wave vectors, we also observed a mode that we interpret as being a longitudinal optic branch, due to the fact that it has an energy gap at the zone center. We have not developed a model for the lattice dynamics of chalcopyrite, since we consider that the data are incomplete at present.

We used the following spin Hamiltonian for analyzing the spin-wave spectra:

$$\mathcal{H} = J \sum_{j,\delta} \mathbf{S}_j \cdot \mathbf{S}_{j+\delta} + D \sum_j (S_{jz})^2, \quad (1)$$

where J is the nearest-neighbor exchange integral, $\mathbf{S}_j = (S_{jx}, S_{jy}, S_{jz})$ is the spin of the j th atom, D is the single-ion anisotropy energy, and the sum for every atom j is over all nearest neighbors δ . For this analysis, we consider only the magnetic moment on the Fe atoms, since the ordered moment on the Cu atoms is negligibly small.³ Using the method of Holstein and Primakoff,^{6,7} and only considering nearest-neighbor interactions between Fe atoms, the dispersion relation for a general coordinate $(h k l)$ in reciprocal lattice units can be approximated as

$$\omega_{(h k l)}^2 \approx 16J^2S^2(4 - \cos^2\pi h - \cos^2\pi k - 2\cos\pi h \cos\pi k \cos\pi l) + \omega_0^2, \quad (2)$$

where ω_0 is the spin-wave gap at the magnetic zone center, due to anisotropy. For wave vectors close to a magnetic zone center, we can approximate this further to

$$\omega_q^2 \approx 4J^2S^2[2a^2(q_x^2 + q_y^2) + c^2q_z^2] + \omega_0^2, \quad (3)$$

where q_x , q_y , and q_z are the reduced wave vectors from the magnetic zone center parallel to the \mathbf{a}^* , \mathbf{b}^* , and \mathbf{c}^* directions, respectively, and a and c are the lattice parameters. We found that for our sample, at room temperature these had the values $a = 5.294 \text{ \AA}$ and $c = 10.446 \text{ \AA}$. The precise value of S is unclear; Donnay *et al.*³ determined the magnetic moment on the Fe atoms in chalcopyrite to be $3.85\mu_B$, which compares well with the measured magnetic moments of other transition ions with $S = 3/2$, such as Cr^{3+} . We adopt this value for S here. The neutron-scattering cross section for transverse spin waves⁸ is

$$\frac{d^2\sigma}{d\Omega d\omega} = \left(\frac{\gamma e^2}{m_e c^2}\right)^2 \frac{N}{\pi(2\mu_B)^2} \frac{k_f}{k_i} |f(\mathbf{Q})|^2 (1 + Q_z^2) \times [n(\omega) + 1] \chi''(\mathbf{Q}, \omega), \quad (4)$$

where k_i and k_f are the incident and scattered neutron wave vectors, respectively, $f(\mathbf{Q})$ is the magnetic form factor, Q_z is the component of the wave-vector transfer parallel to the c^* axis, and $n(\omega) + 1$ is the Bose-Einstein population factor. $\chi''(\mathbf{Q}, \omega)$ is the imaginary part of the susceptibility, and we used the form

$$\chi''(\mathbf{Q}, \omega) = \frac{\Gamma \omega}{\Gamma^2 \omega^2 + (\omega^2 - \omega_q^2)^2}, \quad (5)$$

where Γ is the damping of the spin waves.

The experimental spin-wave data were analyzed by fitting with Eqs. (3) and (4) convoluted with the four-dimensional experimental resolution function, which was calculated at each data point using the method of Popovici, Stoica, and Ionita.⁹ We used the data taken with the high- and low-energy transfer configurations for slightly different purposes: since the splitting of the spin waves on either side of the zone center is only resolvable in a constant-energy scan at relatively high energy transfers (above about 5 THz), the data taken with the low-energy transfer configuration were largely used for determining a precise value for the spin-wave gap ω_0 . Once this was found, the nearest-neighbor exchange J , was determined by fitting Eqs. (3) and (4) to the data from the high-energy transfer configuration. These data consist of a series of constant-energy scans between 5 and 12 THz along two different directions through the $(1 1 4)$ magnetic zone center, and in the fitting procedure we fitted to all of these spectra simultaneously. The only parameters that were varied at this stage were an overall scale factor and J ; the agreement factor obtained was reasonably good ($\chi^2 = 1.6$). We found that the spin-wave gap is $\omega_0 = 1.28(1)$ THz, while the exchange energy is $J = 2.27(2)$ THz. This means that the spin-wave velocity for $[h 0 0]$ wave vectors is $51.0(5)$ THz \AA and $71.2(5)$ THz \AA for $[0 0 l]$ wave vectors. It was found that the intrinsic

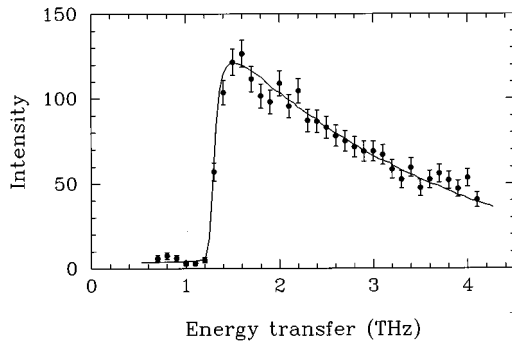


FIG. 2. Constant- Q scan at $Q=(1\ 1\ 0)$ measured with the low-energy transfer configuration. The curve shows a fit to the data of the theoretical scattering function, convoluted with the experimental resolution.

width of the spin-wave branches is too small to measure with our experimental resolution, so the spin-wave damping Γ was kept fixed at the nominal, very small, value of 0.01 THz during the data analysis.

In Fig. 2, we show data taken from a constant- Q scan at the $(1\ 1\ 0)$ magnetic zone center using the low-energy transfer configuration, with the fitted profile shown as the curve. The highly asymmetric profile reflects the way that the resolution ellipsoid intersects with the very steep spin-wave surface. In Fig. 3, we show a series of constant-energy scans across the spin-wave branches around the $(1\ 1\ 4)$ position, taken with the high-energy transfer configuration. The splitting of the branches is clear for scans with $[h\ h\ 4]$ wave vectors, but is barely discernible for the $[1\ 1\ l]$ scans, because of the higher spin-wave velocity.

To summarize, we have studied the phonon and spin-wave dispersion of chalcopyrite (CuFeS_2) under ambient conditions. The spin waves are found to be steeply dispersive, with a gap of 1.28(1) THz at the magnetic zone center, which we suggest is due to single-ion anisotropy. We have analyzed the spin-wave data with a model that only considers

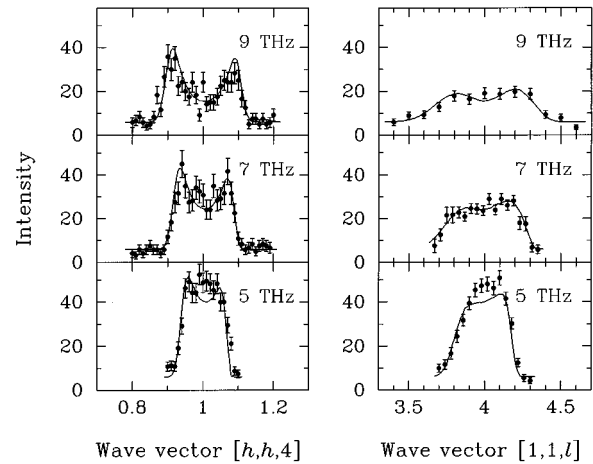


FIG. 3. Constant-energy scans around $Q=(1\ 1\ 4)$, measured with the high-energy transfer configuration. The curves show fits to the data of the theoretical scattering function, convoluted with the experimental resolution.

interactions between nearest-neighboring magnetic ions, and have found good agreement. The magnetic moment of the Fe atoms is known from previous work³ to be reduced from the two possible free-ion values, and using the value $S=3/2$, we determine the exchange energy between nearest neighbors to be $J=2.27(2)$ THz. We conclude that, in spite of the fact that certain electrical and magnetic properties (together with the results of band-structure calculations⁴) indicate that the magnetic Fe 3d electrons are at least partially delocalized, the spin dynamics are consistent with a simple local-moment model.

M.J.H. and M.P.Z. wish to thank the staff of Chalk River Laboratories for their hospitality and the EPSRC for financial support. We are grateful to the Natural History Museum for supplying the single crystal of chalcopyrite used in this study, and to W.J.L. Buyers, T.G. Perring, and P. Verrucchi for helpful discussions.

¹T. Teranishi, K. Sato, and K. Kondo, *J. Phys. Soc. Jpn.* **36**, 1618 (1974).

²T. Teranishi, *J. Phys. Soc. Jpn.* **16**, 1881 (1961).

³G. Donnay, L. M. Corliss, J. D. H. Donnay, N. Elliott, and J. M. Hastings, *Phys. Rev.* **112**, 1917 (1958).

⁴T. Hamajima, T. Kambara, K. I. Gondaira, and T. Oguchi, *Phys. Rev. B* **24**, 3349 (1981).

⁵A. P. Mikhailovskii, A. M. Polubotko, V. D. Prochukhan, and Y.

V. Rud, *Phys. Status Solidi B* **158**, 229 (1990).

⁶T. Holstein and H. Primakoff, *Phys. Rev.* **58**, 1098 (1940).

⁷C. Kittel, *Quantum Theory of Solids* (Wiley, New York, 1987).

⁸S. W. Lovesey, *Theory of Neutron Scattering from Condensed Matter, Vol. 2* (Clarendon, Oxford, 1984).

⁹M. Popovici, A. D. Stoica, and I. Ionita, *J. Appl. Crystallogr.* **20**, 90 (1987).